

## RESEARCH ARTICLE

# Selected reaction monitoring for the quantification of *Escherichia coli* ribosomal proteins

Yuishin Kosaka<sup>1</sup>, Wataru Aoki<sup>1,2\*</sup>, Megumi Mori<sup>1</sup>, Shunsuke Aburaya<sup>1</sup>, Yuta Ohtani<sup>1</sup>, Hiroyoshi Minakuchi<sup>3</sup>, Mitsuyoshi Ueda<sup>1,2</sup>

**1** Division of Applied Life Sciences, Graduate School of Agriculture, Kyoto University, Kyoto, Japan, **2** Kyoto Integrated Science & Technology Bio-Analysis Center, Kyoto, Japan, **3** Kyoto Monotech, Kyoto, Japan

\* [aoki.wataru.6a@kyoto-u.ac.jp](mailto:aoki.wataru.6a@kyoto-u.ac.jp)



## OPEN ACCESS

**Citation:** Kosaka Y, Aoki W, Mori M, Aburaya S, Ohtani Y, Minakuchi H, et al. (2020) Selected reaction monitoring for the quantification of *Escherichia coli* ribosomal proteins. PLoS ONE 15(12): e0236850. <https://doi.org/10.1371/journal.pone.0236850>

**Editor:** John Matthew Koomen, H Lee Moffitt Cancer Center and Research Institute, UNITED STATES

**Received:** July 11, 2020

**Accepted:** November 25, 2020

**Published:** December 14, 2020

**Copyright:** © 2020 Kosaka et al. This is an open access article distributed under the terms of the [Creative Commons Attribution License](https://creativecommons.org/licenses/by/4.0/), which permits unrestricted use, distribution, and reproduction in any medium, provided the original author and source are credited.

**Data Availability Statement:** The datasets generated and/or analyzed during the current study are available in the jPOST repository (accession number: JPST000907 or PXD020266) (<https://repository.jpostdb.org/entry/JPST000907>).

**Funding:** W.A. was supported by the Japan Society for the Promotion of Science (grant No. 19K16109 and 26830139; <https://www.jsps.go.jp/english/>), Sugiyama Chemical & Industrial Laboratory (<http://www.sugiyama-c-i.or.jp/>), and the JGC-S

## Abstract

Ribosomes are the sophisticated machinery that is responsible for protein synthesis in a cell. Recently, quantitative mass spectrometry (qMS) have been successfully applied for understanding the dynamics of protein complexes. Here, we developed a highly specific and reproducible method to quantify all ribosomal proteins (r-proteins) by combining selected reaction monitoring (SRM) and isotope labeling. We optimized the SRM methods using purified ribosomes and *Escherichia coli* lysates and verified this approach as detecting 41 of the 54 r-proteins separately synthesized in *E. coli* S30 extracts. The SRM methods will enable us to utilize qMS as a highly specific analytical tool in the research of *E. coli* ribosomes, and this methodology have potential to accelerate the understanding of ribosome biogenesis, function, and the development of engineered ribosomes with additional functions.

## Introduction

Ribosomes are the sophisticated machinery that synthesize proteins in all organisms. The *Escherichia coli* ribosome is a multimeric protein complex composed of 30S and 50S subunits. The 30S subunit consists of 21 ribosomal proteins (r-proteins) and 16S ribosomal ribonucleic acid (rRNA), whereas the 50S subunit consists of 33 r-proteins, 5S rRNA, and 23S rRNA. The biogenesis of ribosomes is very complex, and several assembly-associated factors are involved in the process [1, 2]. Studies of the function, structure, and assembly of ribosomes have been promoted in part by the reconstitution of the small and large subunits of ribosomes. The functional *E. coli* 30S subunit was first reconstituted by Traub & Nomura in 1968 [3]. Due to the increased complexity of the structure, the reconstitution of the *E. coli* 50S subunit was not achieved until 1974 by Nierhaus & Dohme [4].

These early researchers revealed essential components of today's knowledge about the assembly of ribosomes, which provides the basis of ribosome reconstruction and engineering. Jewett and coworkers [5–8] developed an *in vitro* integrated synthesis, assembly, and translation (iSAT) method that enables the co-activation of rRNA transcription, and the assembly of the transcribed rRNA with r-proteins into functional ribosomes in *E. coli* lysates. In contrast to the iSAT-based ribosome reconstruction, which uses a mixture of r-proteins, previous studies have also reported that individually purified ribosomal components can be reconstructed

Scholarship Foundation (<https://www.jgcs.or.jp/en/>). Kyoto-monotech provided a monolithic column and support in the form of salaries for HM. The funders did not have any additional role in the study design, data collection and analysis, decision to publish, or preparation of the manuscript. The specific roles of these authors are articulated in the 'author contributions' section.

**Competing interests:** Kyoto-monotech provided a monolithic column and support in the form of salaries for HM. This does not alter our adherence to PLOS ONE policies on sharing data and materials.

into 30S subunits [9–12]. These approaches were integrated in a single reaction in the protein synthesis using recombinant elements (PURE) system [13], which coupled the transcription of 16S rRNA, assembly of the 30S subunit, and synthesis of sfGFP, which was translated by reconstructed ribosomes [14]. Moreover, the autonomous synthesis and assembly of the 30S subunit on a chip using ribosomal genes was reported recently [15].

In parallel to these efforts on ribosome reconstruction, researchers have tried to redesign the translational machinery. Orthogonal translation systems based on modified Shine Dalgarno (SD)/anti-SD sequence pairs enable the translation of orthogonal mRNAs independent of the cellular translation system [16–19]. This strategy has been applied to improving the site-specific incorporation efficiency of unnatural amino acids [20–23] and evaluating the activity of reconstructed or engineered ribosomes [14, 19, 24–26]. In addition, tethered or stapled approaches [19, 24–27] have been established to facilitate the engineering of 50S subunits. Analyzing the structure-function correlation when mutations are introduced to the peptidyl transferase center (PTC) is also a target of ribosome engineering [28, 29], and a recent study established a high-throughput evaluation system using iSAT to evaluate comprehensive mutations in PTCs [30]. The artificial evolution of 16S rRNA for the reconstruction of functional 30S subunits without post-transcriptional modifications is also achieved by combining iSAT, *in vitro* evolution, and a liposome sorting technique [31].

It is valuable to analyze the dynamics of each component to understand the process of ribosome reconstruction. For example, tracking expression levels or incorporation rates of each r-protein into ribosome assembly intermediates provides crucial information toward understanding the assembly process. Previous studies used quantitative mass spectrometry (qMS) to reveal the composition of r-proteins and associated factors of ribosome assembly intermediates [2, 32, 33] and the stoichiometry of components of reconstructed ribosomes [12, 14, 26]. Among various qMS approaches, selected reaction monitoring (SRM), which enables specific quantification of trace amounts of targeted proteins [34], can be a powerful method to accelerate the reconstruction and engineering of ribosomes. However, SRM methods have been developed for a limited number of r-proteins [35] and not for all 54 *E. coli* r-proteins.

In this study, we developed a highly specific method to quantify all *E. coli* r-proteins by combining targeted proteomics using SRM with isotope labeling of nascent r-proteins. We determined optimized transitions for the quantification of 54 r-proteins using protein digests of purified ribosomes, *E. coli* lysate, and r-protein-overexpressed *E. coli* lysates. Further, we verified the SRM methods as a high-throughput analytical tool by detecting 41 of the 54 r-proteins separately synthesized in *E. coli* S30 extracts. This method will enable the utilization of the SRM methods as a highly specific analytical tool in the field of ribosome research, and it has the potential to accelerate the understanding of ribosome biogenesis and development of functionally modified ribosomes (Fig 1).

## Materials and methods

### Plasmids and strains

Genes encoding ribosomal proteins were amplified from the complete set of *E. coli* K-12 ORF archive (ASKA) library [36], and a vector backbone was amplified by PCR using pUC19 with KOD-Plus-Neo (TOYOBO, Osaka, Japan). The amplified fragments were gel-purified and fused using an In-Fusion<sup>®</sup> HD Cloning Kit (Takara Bio, Shiga, Japan). Full sequences of the plasmids used in this study are provided in S1 File. In terms of the plasmids encoding each r-protein, we showed the sequence of pT7\_rplA as a representative (S1 File).

The chromosomal *lacZ* gene of BL21 Star<sup>™</sup> (DE3) (Thermo Fisher Scientific, Waltham, MA, USA) was replaced with the kanamycin-resistance gene (*kmr*) using Red-mediated

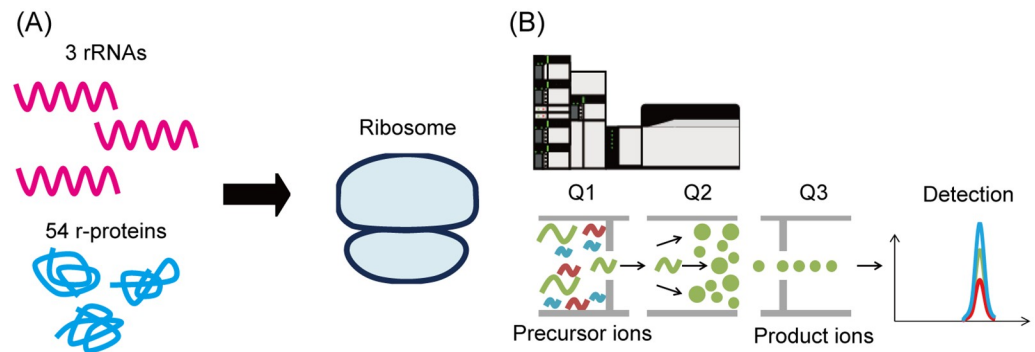


**Fig 1. Selected reaction monitoring analysis for the quantification of *Escherichia coli* ribosomal proteins.** (A) Biogenesis of *E. coli* ribosomes, including the assembly of three rRNAs and 54 r-proteins. (B) Nascent r-proteins and endogenous r-proteins were quantified using optimized SRM methods. The SRM methods enable us to utilize qMS as a high-throughput hypothesis testing tool for the research of *E. coli* ribosomes.

<https://doi.org/10.1371/journal.pone.0236850.g001>

recombination [37]. The Red helper plasmid, pKD46, was transformed into the *E. coli* cells, and the transformants were cultured in 50 mL SOC medium with 100  $\mu\text{g}/\text{ml}$  ampicillin (Vic-cillin<sup>®</sup> for injection, Meiji Seika Pharma, Tokyo, Japan) and 10 mM L-(+)-arabinose (Nacalai Tesque, Kyoto, Japan). The fragment of the *kmr* gene was amplified using primers from pKD13: the H1P1 forward primer, 5' - GAAATTGTGAGCGGATAACAATTCACACAG GAAACAGCTGTGTAGGCTGGAGCTGCTTC-3', and the P4H2 reverse primer, 5' -TTACGC GAAATACGGGCAGACATGGCCTGCCCGTTATTAATTCGGGGATCCGTCGACC-3'. Then, it was purified using a MinElute<sup>®</sup> PCR Purification Kit (QIAGEN, Hilden, Germany). Electroporation was performed using a Gene Pulser<sup>®</sup> II (Bio-Rad, Hercules, CA, USA) with a Nepa Electroporation Cuvette with a 1 mm gap (Nepa Gene, Chiba, Japan) at 1350 V, 10  $\mu\text{F}$ , and 600 Ohm. Next, the electroporated cells were incubated overnight at room temperature in SOC medium. After incubation, the cells were cultured on an LB agar plate containing 50  $\mu\text{g}/\text{ml}$  kanamycin monosulfate (Nacalai Tesque) to select Km<sup>R</sup> transformants. The deletion of the *lacZ* gene was verified using blue-white selection on an LB agar plate containing 0.1 mM isopropyl- $\beta$ -D-thiogalactopyranoside (Nacalai Tesque) and  $4.0 \times 10^{-3}\%$  5-bromo-4-chloro-3-indolyl- $\beta$ -D-galactoside (Takara Bio).

The Miraprep method [38] was performed using LaboPass<sup>™</sup> Plasmid Mini (Hokkaido System Science, Hokkaido, Japan) to prepare plasmids for cell-free protein synthesis (CFPS). Then, the extracted plasmids were purified further using a QIAquick<sup>®</sup> PCR Purification Kit (QIAGEN).

### Preparation of S30 extract

S30 extract was prepared as previously reported [5–7]. BL21 Star<sup>™</sup> (DE3) *lacZ::kmr* cells were grown in 1 L of 2 $\times$ YPTG medium. Then, the cells were disrupted using an EmulsiFlex-C5 homogenizer (Avestin, Ottawa, Canada) with a single pass at a pressure of 20,000 psi. The lysate was centrifuged twice at 30,000  $g$  for 30 min at 4  $^{\circ}\text{C}$ . Then, the supernatant was dialyzed using an iSAT buffer according to previous reports [7, 39]. The protein concentration of the S30 extract was concentrated to 30–40 mg/mL, as determined using a Protein Assay BCA Kit (Nacalai Tesque).

### Cell-free protein synthesis

Cell-free protein synthesis was conducted according to previous reports with slight modifications [5, 8]. The final concentration of T7 RNA polymerase (New England BioLabs, Ipswich,

MA, USA) was 0.8 U/ $\mu$ L. Plasmid concentrations of pET41a\_T7\_sfGFP, pUC19\_T7\_LacZ, and the plasmids encoding ribosomal proteins were 80 nM, 60 nM, and 55.3 nM, respectively. The expression of sfGFP [40] from the pET41a\_T7\_sfGFP plasmid was induced using 2 mM of isopropyl- $\beta$ -D-thiogalactopyranosides. CFPS solutions (15  $\mu$ L) were incubated at 37 °C for 3 h in a black-walled, polystyrene 96-well plate with a solid bottom and half volume (Greiner Bio-One International GmbH, Kremsmünster, Austria). The expression of sfGFP and LacZ was monitored using a Fluoroskan Ascent FL™ 96-well-plate reader (Thermo Fisher Scientific) at  $\lambda_{\text{ex}} = 485$  nm and  $\lambda_{\text{em}} = 510$  nm. To quantify the activity of lacZ, 3.3 nM of 5-chloromethylfluorescein di-beta-D-galactopyranoside (CMFDG) (Invitrogen, Waltham, MA, USA) was added to the reaction solution. For isotope labeling, we used 20 amino acids that contained 2 mM of  $^{13}\text{C}_6$   $^{15}\text{N}_2$  L-lysine (Thermo Fisher Scientific) and  $^{13}\text{C}_6$   $^{15}\text{N}_4$  L-arginine (Thermo Fisher Scientific) instead of  $^{12}\text{C}_6$   $^{14}\text{N}_2$  L-lysine and  $^{12}\text{C}_6$   $^{14}\text{N}_4$  L-arginine (Sigma-Aldrich Corporation, St. Louis, MO, USA). The synthesized proteins were quantified using a liquid chromatograph-triple quadrupole mass spectrometer LCMS-8060 (Shimadzu, Kyoto, Japan), as described below.

### Overexpression of r-proteins in *Escherichia coli*

The plasmids encoding each ribosomal protein were purified using the ASKA library [36]. Then, the plasmids were introduced into *E. coli* BL21 (DE3) *lacZ::kmr*. The cells were grown at 37 °C to  $\text{OD}_{600} = 0.5$ – $0.6$  in 5 mL LB medium containing 100  $\mu\text{g}/\text{ml}$  ampicillin (Viccillin® for injection, Meiji Seika Pharma), incubated at 37 °C for 3 h with 0.1 or 1 mM IPTG (Nacalai tesque), and then centrifuged at 3,000 rpm for 5 min. Then, the pellets of the cells were suspended in 200  $\mu\text{L}$  of lysis buffer of 2 M urea, 50 mM ammonium bicarbonate, and with a pH of 8.0 and transferred into 1.5 mL microtubes in an ice-water bath. The cells were disrupted using a sonicator (BIORUPTOR UCD-250, Cosmo Bio, Tokyo, Japan) for 10 min at 4 °C (Level 5, a 30-s sonication with 30-s interval). Then, the lysates were centrifuged at 14,000 g for 10 min at 4 °C, and the supernatants were collected. The ribosomal proteins were quantified using the LCMS-8060 (Shimadzu, Kyoto, Japan) as described below.

### Preparation of protein digests

The protein samples of purified ribosome (New England BioLabs), *E. coli* lysate, *E. coli* lysates containing each overexpressed r-protein, r-proteins produced in S30 extract, and LacZ produced in S30 extract were mixed with 120  $\mu\text{L}$  of methanol, 30  $\mu\text{L}$  of chloroform, and 90  $\mu\text{L}$  of ultrapure water, which were added to 30  $\mu\text{L}$  of each protein sample and vortexed thoroughly. Then, the mixtures were centrifuged at 13,000 g for 5 min. The top aqueous layer was pipetted off, and 90  $\mu\text{L}$  of methanol was added to the solution. Then, the solution was mixed thoroughly and centrifuged at 13,000 g for 5 min. The aqueous layer was pipetted off and the pellet was air-dried for 5 min. Then, the pellet was dissolved in a lysis buffer of 2 M urea and 50 mM ammonium bicarbonate with a pH of 8.0. After alkylation and reduction steps [41], proteolytic enzymes, trypsin (Promega, Madison, WI, USA) and/or lysyl endopeptidase (FUJIFILM Wako Pure Chemical Corporation, Osaka, Japan) were added to the samples at the ratio of total proteins/proteolytic enzyme = 75:1 (w/w). The samples were shaken at 37 °C for 24 h, and then the reaction was stopped by adding trifluoroacetic acid to provide a final concentration of 1% (v/v). The digested peptides were desalted using a MonoSpin® C18 column (GL Sciences, Tokyo, Japan) and dried using vacuum centrifugation. Then, the dried samples were reconstituted to 5  $\mu\text{g}/\mu\text{L}$  using 10% formic acid. Next, the peptide samples were filtered through 0.45  $\mu\text{m}$  filters (Merck KGaA, Darmstadt, Germany). For the digestion of rplF, rplT, rplY, and rpmC that were synthesized in S30 extracts, samples were digested using Lys-C for 4

h, and then they were digested using trypsin for 24 h. The same enzyme-to-substrate ratio (75:1) was used when digesting with both Lys-C and trypsin.

### Quantification of ribosomal proteins using a liquid chromatography-selected reaction monitoring mass spectrometry

The digested proteins were analyzed using an UltiMate 3000 RSLCnano (Thermo Fisher Scientific) and an LCMS-8060 (Shimadzu, Kyoto, Japan) triple quadrupole mass spectrometer. A 500 mm monolithic column with a 100  $\mu\text{m}$  ID [42] was connected to a six-port injection/switching valve (Valco Instruments, Houston, TX, USA). A 5  $\mu\text{m}$ , 0.3 $\times$ 5 mm L-column ODS (Chemical Evaluation and Research Institute, Saitama, Japan) was used as a trap column. The samples were passed through a 20  $\mu\text{L}$  sample loop and injected into the monolithic column at a flow rate of 500 nL/min. Then, a gradient was generated by varying the mixing ratio of the two eluents: 0.1% (v/v) formic acid diluted with ultrapure water (eluent A); and 0.1% (v/v) formic acid diluted with acetonitrile (eluent B). The gradient started at 5% of eluent B over 7.5 min, it was then increased to 40% of eluent B for 27.5 min, and it was finally increased to 95% of eluent B for a 5-min hold. Then, the ratio of eluent B was quickly adjusted to the initial composition and held for 5 min to re-equilibrate the column. The column oven was kept at 40  $^{\circ}\text{C}$ , and the autosampler was kept at 4  $^{\circ}\text{C}$ . The block and the interface temperature were adjusted to 400  $^{\circ}\text{C}$  and 300  $^{\circ}\text{C}$ , respectively. Using Skyline software [43], we prepared SRM methods for both non-labeled proteins and proteins that were labeled with  $^{13}\text{C}_6$   $^{15}\text{N}_2$  L-lysine and  $^{13}\text{C}_6$   $^{15}\text{N}_4$  L-arginine. Doubly and triply charged states of 6–25 mer peptides were selected to predict precursor ion candidates. Peptides, including methionine, were excluded from the candidates because they are susceptible to oxidation and unsuitable for quantitative analysis. Carbamidomethyl cysteine was set as a fixed modification. For fragment ions, singly charged or doubly charged b- or y-series ions with 50–1500 m/z were predicted. All selected peptides were evaluated for the uniqueness of their sequences using an *E. coli* background, and the SRM methods were scheduled based on the obtained retention time with a dwell time of 5 ms.

### Data analysis

We analyzed protein digests of purified ribosome (New England BioLabs) and purified LacZ (FUJIFILM Wako Pure Chemical Corporation) and drew calibration curves to quantify the r-proteins and LacZ synthesized in S30 extracts. Up to three quantitative transitions were selected for r-proteins and six transitions were selected for LacZ. As for the quality control metrics, r-proteins with S/N ratio over 5 was defined as detected. The relative amount of each r-protein was quantified using a single transition with the highest S/N ratio among the selected transitions. We calculated the ratio of peak areas from isotope-labeled 'heavy' r-proteins and 'light' endogenous r-proteins to compare the abundance ratio of r-proteins synthesized in S30 extracts to the endogenous counterparts. The names of r-proteins were written according to the universal nomenclature for r-proteins [44]. The datasets generated and/or analyzed during the current study are available in the jPOST repository (accession number: JPST000907 or PXD020266) [45]. Statistical analysis was conducted using a two-tailed *t*-test.

## Results

### Development of selected reaction monitoring methods for the quantification of r-proteins

For the SRM analysis, we selected peptides that met the following criteria: (1) peptides that show intense peaks when prepared using purified ribosomes, (2) peptides that show intense

peaks when prepared using *E. coli* lysate and show the same retention times observed at (1), and (3) peptides that show stronger intensities when prepared using r-protein-overexpressed *E. coli* lysates compared with that of (2). We attempted to select three peptides for each r-protein and 3–4 fragment ions for each peptide to enable precise quantification.

We predicted precursor-to-fragment ion transitions using Skyline for each protein of interest, analyzed the protein digests prepared using purified ribosomes, and selected candidate transitions for each r-protein (S1 Fig). The selected transitions were then verified by analyzing the protein digests prepared using *E. coli* lysate or r-protein-overexpressed *E. coli* lysates, as described in the Materials and methods section (S1 Fig). We successfully selected specific transitions for each r-protein, as seen in S2 Fig and S1 Table, and the optimized SRM methods are summarized in S2 Table. The linearity of the SRM methods was determined using a dilution series of protein digests of purified ribosomes. A dilution rate of 1.0 represents a 5  $\mu$ L injection of 8  $\mu$ g/mL of the samples. The peak area of each peptide was plotted against its concentration, and most transitions showed a high correlation coefficient (S3 Table).

### Evaluation of cell-free protein synthesis using S30 extracts

We attempted to quantify r-proteins separately produced in *E. coli* S30 extracts using our SRM methods as a high-throughput analytical tool. To evaluate the activity of the *E. coli* S30 extracts, we produced sfGFP in the *E. coli* S30 extract, and achieved a reaction yield of about 2.0 mg/mL (S3 Fig), which is comparable to that of previous reports [6, 39]. To evaluate the production level of r-proteins, we discriminated nascent r-proteins from endogenous r-proteins. Then, we planned to incorporate isotope-labeled amino acids into the nascent r-proteins. However, endogenous amino acids in S30 extracts can also be incorporated into nascent r-proteins. Therefore, we determined the incorporation rates of endogenous and exogenous amino acids into the nascent proteins. As a model, we attempted to quantify the incorporation rates of isotope-labeled amino acids into the LacZ that was synthesized in S30 extracts derived from the *E. coli* BL21 Star™ (DE3) *lacZ::kmr* strain. First, we developed SRM methods for LacZ with high specificity and accuracy (S4 Fig and S4 and S5 Tables). Then, we synthesized LacZ in the S30 extracts with or without isotope-labeled amino acids, and we determined peptide ratios of heavy to light (Fig 2). Consequently, we found that most of the nascent LacZ consisted of only

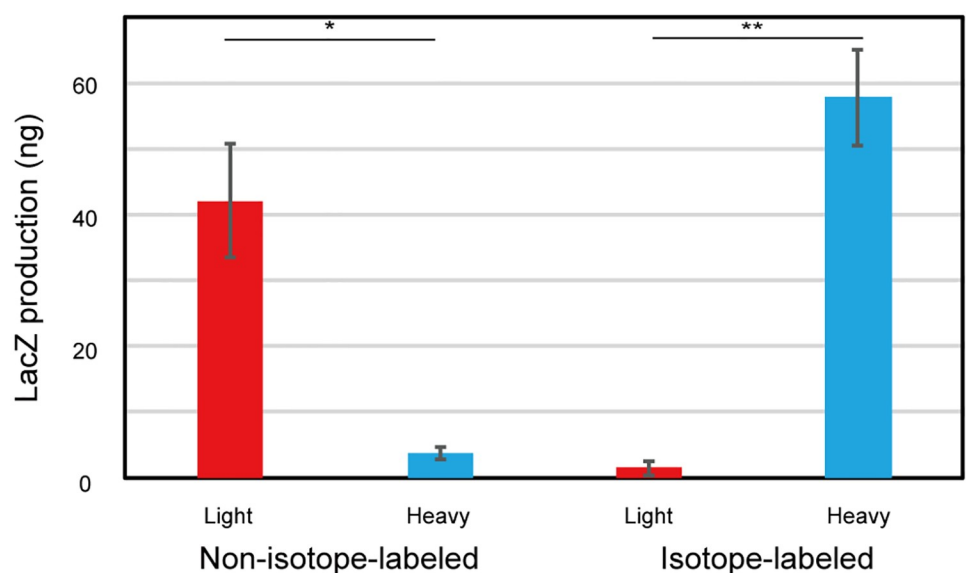


**Fig 2. Quantification of LacZ synthesized in S30 extract.**

<https://doi.org/10.1371/journal.pone.0236850.g002>

isotope-labeled amino acids. This is because the cell lysates were dialyzed using an iSAT buffer, which washed out almost all of the endogenous amino acids. These results suggest that the intensity of the 'heavy' peptides directly corresponds to the protein production level in the S30 extracts that were prepared in this study.

Quantification of LacZ synthesized with or without 2 mM of  $^{13}\text{C}_6$   $^{15}\text{N}_2$  L-lysine and  $^{13}\text{C}_6$   $^{15}\text{N}_4$  L-arginine in S30 extracts. The protein digests were quantified using the selected reaction monitoring methods for LacZ and we used four peptides (GDFQFNISR, IGLNCQLAQAER, IDPNAWVER, and DWENPGVTQLNR) for LacZ quantification. The protein yield was deduced based on the peak area of the transitions. A non-isotope-labeled control was used to measure background signals. Data are shown as mean  $\pm$  standard error. The mean values were calculated based on triplicate analysis. Statistical significance was determined using a two-tailed Student's *t*-test with significance at \**p* < 0.05, \*\**p* < 0.01. The blue bar indicates heavy proteins and the red bar indicates light proteins.

### Profiling of nascent r-proteins separately produced in S30 extracts

To confirm whether nascent r-proteins can be labeled by isotope and detected by the SRM methods, each r-protein was separately synthesized in S30 extracts containing 2 mM of  $^{13}\text{C}_6$   $^{15}\text{N}_2$  L-lysine and  $^{13}\text{C}_6$   $^{15}\text{N}_4$  L-arginine instead of  $^{12}\text{C}_6$   $^{14}\text{N}_2$  L-lysine and  $^{12}\text{C}_6$   $^{14}\text{N}_4$  L-arginine. The S30 extracts were digested and analyzed as described in the Materials and methods section, and the ratios of nascent r-proteins ('heavy') to endogenous r-proteins ('light') were calculated (Heavy/Light ratio) to investigate the abundance ratio of nascent proteins to endogenous counterparts. The r-proteins, which had an S/N ratio >5 were defined as detected proteins (Fig 3 and S6 Table). As a result, 41 of the 54 'heavy' r-proteins were successfully detected while the others were undetected: bL21, bL27, uL30, bL31, bL34, bL35, uS2, uS7, uS8, uS13, bS16, uS19, and bS21. Although several r-proteins showed higher intensity peaks, many of the detected r-proteins had lower intensity peaks than their endogenous counterparts probably because of their lower abundance of the nascent r-proteins in S30 extracts and the limited number of peptide candidates for SRM analysis.

### Discussion

qMS has been successfully applied for understanding ribosome biogenesis and the development of functionally modified ribosomes. For example, qMS was used to measure relative production levels of r-proteins [46], and more recently, has revealed the composition of r-proteins and associated factors of ribosome assembly intermediates [2, 32, 33]. A flexible standard has also been developed using QconCAT technology to capture the composition of stable or transient ribosome complexes using orbitrap and MALDI-TOF mass spectrometry [47]. Furthermore, qMS approach has been used for analyzing *in vitro* ribosome reconstruction [12, 14] and ribosome engineering [48].

In parallel to the previous studies, SRM, which enables highly specific quantification of targeted proteins, can serve an alternative mass spectrometric approach [49]. SRM using triple quadrupole MS can detect and quantify specific ions by setting a combination of *m/z* of a first quadrupole (Q1) filter that passes precursor ions and a third quadrupole (Q3) filter that passes fragment ions after collision-induced dissociation. Normally, multiple transitions (Q3) are set for a single peptide (Q1). Hence, these multiple transitions are detected as co-eluting peaks in a chromatogram, which can guarantee their specificity [34, 50–52]. It is worth noting that SRM can suffer from interference over co-elution of several peptides compared to high resolution MS/MS, which can provide more confidence in such a situation [53].

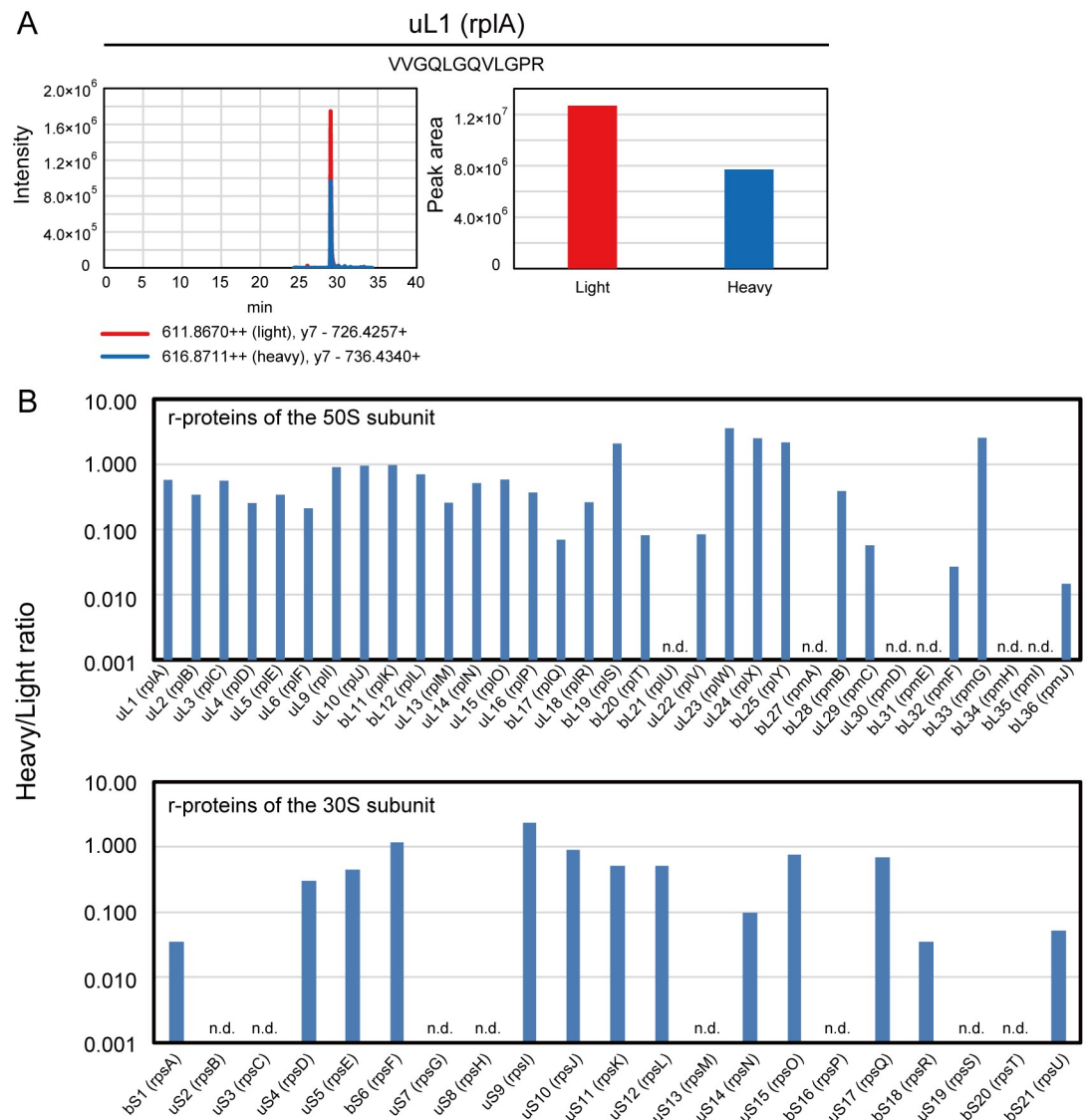


**Fig 3. Quantification of r-proteins synthesized in S30 extracts.** Isotope-labeled r-proteins were separately synthesized in S30 extracts and digested using trypsin or lysyl endopeptidase. The digests were quantified using optimized selected reaction monitoring methods. (A) The chromatogram and peak area of the VVGQLGQVLGPR peptide of uL1 (rplA) for the heavy and light peptides as a representative data from Skyline. Signal intensities for the heavy and light peptides of all r-proteins were shown in S6 Table. (B) The ratios of nascent r-proteins ('heavy') to endogenous r-proteins ('light') were calculated (Heavy/Light ratio). The r-proteins with a S/N ratio >5 were defined as detected proteins. The blue bar indicates detected proteins and n.d. indicates non-detected proteins. The data was based on a single analysis.

<https://doi.org/10.1371/journal.pone.0236850.g003>

So far, SRM methods have been developed against the limited number of r-proteins [35], and not against all 54 *E. coli* r-proteins. In this study, we developed a method to quantify all of the *E. coli* r-proteins with high specificity by combining SRM with isotope labeling of nascent r-proteins. We determined optimized transitions for the quantification of 54 r-proteins using protein digests of purified ribosomes, *E. coli* lysate, and r-protein-overexpressed *E. coli* lysates (S2 Table). The quantification of isotope-labeled LacZ synthesized in S30 extracts derived from an *E. coli lacZ::kmr* strain confirmed that nascent proteins were specifically labeled by isotope amino acids, which enabled precise quantification of nascent proteins (Fig 2). We

verified the SRM approach developed in this study as a high-throughput analytical tool by quantifying all of the r-proteins separately synthesized in *E. coli* S30 extracts.

Some of the r-proteins were not detected when we separately expressed them in S30 extracts: bL21, bL27, uL30, bL31, bL34, bL35, uS2, uS7, uS8, uS13, bS16, uS19, and bS21. These r-proteins included r-proteins smaller than 9 kDa, such as uS2, uS7, uS8, and uS13, which are assumed to be difficult to use for selecting peptides for SRM partly because only a limited number of peptide candidates can be generated from small r-proteins. This problem can be resolved by using proteases other than trypsin or lysyl endopeptidase. In addition, bL17, bL20, bL29, bL36, bS1, and bS21 showed a low expression level, as reported previously [12]. The inefficient expression of some r-proteins can be improved by increasing the translation and protein folding efficiency in S30 extracts by using optimized plasmid design [54], polycistronic expression [55] and the macromolecular crowding effect [56]. Moreover, a pipette-based peptide micropurification system, which enables the multidimensional fractionation, desalting, filtering, and concentration [57] of peptides from reacted S30 extracts, might improve the detection sensitivity of these peptides.

In this study, we did not develop SRM methods for ribosomal peptides with post translational modifications (PTMs). In previous studies, r-proteins are known to be differentially modified in response to different stimuli [58, 59]. In further studies, the development of SRM methods for ribosomal peptides with PTMs will provide us valuable biological implications on ribosomal functions.

In conclusion, we developed a highly specific qMS methods for 54 *E. coli* r-proteins by combining SRM with isotope labeling of nascent r-proteins. The SRM methods for r-proteins established in this study enable the profiling of ribosome biogenesis by quantifying each r-protein in a highly quantitative manner, and they enable us to utilize qMS as a high-throughput hypothesis testing tool in the field of ribosome research. This study provides a powerful method for understanding ribosome biogenesis, and it accelerates research on the reconstruction or engineering of *E. coli* ribosomes.

## Supporting information

**S1 Fig. Ion chromatograms corresponding to peptides derived from r-proteins.** Candidate peptides for selected reaction monitoring analysis were selected using Skyline software. We quantified the prepared r-proteins using purified ribosomes, *E. coli* lysate, and r-protein-over-expressed *E. coli* lysates using a liquid chromatograph-triple quadrupole mass spectrometer. (PDF)

**S2 Fig. Ion chromatograms corresponding to the selected transitions associated with peptides from ribosomal proteins.** For each peptide, several transitions with intense peaks were selected based on the quantification of r-proteins from purified ribosomes. The calibration curves of all transitions are described in S3 Table. The whole peaks of all transition were provided in S1 Table. (PDF)

**S3 Fig. Validation of the protein production activity of S30 extracts.** sfGFP was expressed in S30 extracts prepared using an EmulsiFlex-C5 homogenizer. The expression of sfGFP was monitored using a 96-well-plate reader at  $\lambda_{\text{ex}} = 485$  nm and  $\lambda_{\text{em}} = 510$  nm. Data are shown as the mean  $\pm$  standard error of the mean (N = 3). (TIF)

**S4 Fig. Development of selected reaction monitoring methods for LacZ.** (A) An ion chromatogram corresponding to the transitions associated with peptides from LacZ. Tryptic

digests of LacZ standard were analyzed by a liquid chromatograph-triple quadrupole mass spectrometer. (B) Ion chromatograms corresponding to the selected transitions associated with peptides from LacZ. Tryptic digests of LacZ standard were quantified using triple quadrupole LC-MS/MS, and transitions with intense peak were selected. The whole peaks of all transition were provided in [S4 Table](#). (C) Calibration curves of transitions for the quantification of LacZ.

(TIF)

**S1 Table. Whole peaks corresponding to the selected transitions associated with ribosomal proteins.**

(XLSX)

**S2 Table. Selected reaction monitoring methods for r-proteins.**

(XLSX)

**S3 Table. Calibration curves of selected reaction monitoring methods for r-proteins.**

(XLSX)

**S4 Table. Whole peaks corresponding to selected transitions associated with LacZ.**

(XLSX)

**S5 Table. Selected reaction monitoring methods for LacZ.**

(XLSX)

**S6 Table. Signal intensities for the heavy and light peptides of r-proteins.**

(XLSX)

**S1 File.**

(PDF)

## Acknowledgments

We thank the National BioResource Project (NBRP: *E. coli*) for providing the ASKA library.

## Author Contributions

**Conceptualization:** Wataru Aoki, Megumi Mori, Shunsuke Aburaya.

**Data curation:** Yuishin Kosaka, Wataru Aoki, Megumi Mori.

**Formal analysis:** Yuishin Kosaka, Wataru Aoki, Megumi Mori.

**Funding acquisition:** Wataru Aoki.

**Investigation:** Yuishin Kosaka, Megumi Mori.

**Methodology:** Yuishin Kosaka, Wataru Aoki, Megumi Mori, Shunsuke Aburaya, Yuta Ohtani.

**Project administration:** Yuishin Kosaka, Wataru Aoki, Megumi Mori, Mitsuyoshi Ueda.

**Resources:** Hiroyoshi Minakuchi.

**Supervision:** Wataru Aoki.

**Validation:** Yuishin Kosaka, Wataru Aoki, Megumi Mori.

**Visualization:** Yuishin Kosaka, Wataru Aoki, Megumi Mori.

**Writing – original draft:** Yuishin Kosaka, Wataru Aoki, Megumi Mori.

**Writing – review & editing:** Yuishin Kosaka, Wataru Aoki, Megumi Mori, Shunsuke Aburaya, Yuta Ohtani, Hiroyoshi Minakuchi, Mitsuyoshi Ueda.

## References

1. Kaczanowska M, Ryden-Aulin M. Ribosome biogenesis and the translation process in *Escherichia coli*. *Microbiol Mol Biol Rev*. 2007; 71(3):477–94. Epub 2007/09/07. <https://doi.org/10.1128/MMBR.00013-07> PMID: 17804668.
2. Chen SS, Williamson JR. Characterization of the ribosome biogenesis landscape in *E. coli* using quantitative mass spectrometry. *J Mol Biol*. 2013; 425(4):767–79. Epub 2012/12/12. <https://doi.org/10.1016/j.jmb.2012.11.040> PMID: 23228329.
3. Traub P, Nomura M. Structure and function of *E. coli* ribosomes. V. Reconstitution of functionally active 30S ribosomal particles from RNA and proteins. *Proc Natl Acad Sci U S A*. 1968; 59(3):777–84. Epub 1968/03/01. <https://doi.org/10.1073/pnas.59.3.777> PMID: 4868216.
4. Nierhaus KH, Dohme F. Total reconstitution of functionally active 50S ribosomal subunits from *Escherichia coli*. *Proc Natl Acad Sci U S A*. 1974; 71(12):4713–7. Epub 1974/12/01. <https://doi.org/10.1073/pnas.71.12.4713> PMID: 4612527.
5. Jewett MC, Fritz BR, Timmerman LE, Church GM. In vitro integration of ribosomal RNA synthesis, ribosome assembly, and translation. *Mol Syst Biol*. 2013; 9:678. Epub 2013/06/27. <https://doi.org/10.1038/msb.2013.31> PMID: 23799452.
6. Fritz BR, Jewett MC. The impact of transcriptional tuning on in vitro integrated rRNA transcription and ribosome construction. *Nucleic Acids Res*. 2014; 42(10):6774–85. Epub 2014/05/06. <https://doi.org/10.1093/nar/gku307> PMID: 24792158.
7. Fritz BR, Jamil OK, Jewett MC. Implications of macromolecular crowding and reducing conditions for in vitro ribosome construction. *Nucleic Acids Res*. 2015; 43(9):4774–84. Epub 2015/04/22. <https://doi.org/10.1093/nar/gkv329> PMID: 25897121.
8. Caschera F, Karim AS, Gazzola G, d'Aquino AE, Packard NH, Jewett MC. High-Throughput Optimization Cycle of a Cell-Free Ribosome Assembly and Protein Synthesis System. *ACS Synth Biol*. 2018; 7(12):2841–53. Epub 2018/10/26. <https://doi.org/10.1021/acssynbio.8b00276> PMID: 30354075.
9. Culver GM, Noller HF. Efficient reconstitution of functional *Escherichia coli* 30S ribosomal subunits from a complete set of recombinant small subunit ribosomal proteins. *RNA*. 1999; 5(6):832–43. Epub 1999/06/22. <https://doi.org/10.1017/s1355838299990714> PMID: 10376881.
10. Maki JA, Schnobrich DJ, Culver GM. The DnaK chaperone system facilitates 30S ribosomal subunit assembly. *Mol Cell*. 2002; 10(1):129–38. Epub 2002/08/02. [https://doi.org/10.1016/s1097-2765\(02\)00562-2](https://doi.org/10.1016/s1097-2765(02)00562-2) PMID: 12150913.
11. Tamaru D, Amikura K, Shimizu Y, Nierhaus KH, Ueda T. Reconstitution of 30S ribosomal subunits in vitro using ribosome biogenesis factors. *RNA*. 2018; 24(11):1512–9. Epub 2018/08/05. <https://doi.org/10.1261/rna.065615.118> PMID: 30076205.
12. Li J, Haas W, Jackson K, Kuru E, Jewett MC, Fan ZH, et al. Cogenerating Synthetic Parts toward a Self-Replicating System. *ACS Synth Biol*. 2017; 6(7):1327–36. Epub 2017/03/24. <https://doi.org/10.1021/acssynbio.6b00342> PMID: 28330337.
13. Shimizu Y, Inoue A, Tomari Y, Suzuki T, Yokogawa T, Nishikawa K, et al. Cell-free translation reconstituted with purified components. *Nat Biotechnol*. 2001; 19(8):751–5. Epub 2001/08/02. <https://doi.org/10.1038/90802> PMID: 11479568.
14. Shimojo M, Amikura K, Masuda K, Kanamori T, Ueda T, Shimizu Y. In vitro reconstitution of functional small ribosomal subunit assembly for comprehensive analysis of ribosomal elements in *E. coli*. *Commun Biol*. 2020; 3(1):142. Epub 2020/03/28. <https://doi.org/10.1038/s42003-020-0874-8> PMID: 32214223.
15. Levy M, Falkovich R, Daube SS, Bar-Ziv RH. Autonomous synthesis and assembly of a ribosomal subunit on a chip. *Sci Adv*. 2020; 6(16):eaaz6020. Epub 2020/06/05. <https://doi.org/10.1126/sciadv.aaz6020> PMID: 32494616.
16. Rackham O, Chin JW. A network of orthogonal ribosome x mRNA pairs. *Nat Chem Biol*. 2005; 1(3):159–66. Epub 2006/01/13. <https://doi.org/10.1038/nchembio719> PMID: 16408021.
17. Shine J, Dalgarno L. The 3'-terminal sequence of *Escherichia coli* 16S ribosomal RNA: complementarity to nonsense triplets and ribosome binding sites. *Proc Natl Acad Sci U S A*. 1974; 71(4):1342–6. Epub 1974/04/01. <https://doi.org/10.1073/pnas.71.4.1342> PMID: 4598299.
18. Chubiz LM, Rao CV. Computational design of orthogonal ribosomes. *Nucleic Acids Res*. 2008; 36(12):4038–46. Epub 2008/06/05. <https://doi.org/10.1093/nar/gkn354> PMID: 18522973.

19. Carlson ED, d'Aquino AE, Kim DS, Fulk EM, Hoang K, Szal T, et al. Engineered ribosomes with tethered subunits for expanding biological function. *Nat Commun.* 2019; 10(1):3920. Epub 2019/09/04. <https://doi.org/10.1038/s41467-019-11427-y> PMID: 31477696.
20. Wang K, Neumann H, Peak-Chew SY, Chin JW. Evolved orthogonal ribosomes enhance the efficiency of synthetic genetic code expansion. *Nat Biotechnol.* 2007; 25(7):770–7. Epub 2007/06/27. <https://doi.org/10.1038/nbt1314> PMID: 17592474.
21. Neumann H, Wang K, Davis L, Garcia-Alai M, Chin JW. Encoding multiple unnatural amino acids via evolution of a quadruplet-decoding ribosome. *Nature.* 2010; 464(7287):441–4. Epub 2010/02/16. <https://doi.org/10.1038/nature08817> PMID: 20154731.
22. Wang K, Sachdeva A, Cox DJ, Wilf NM, Lang K, Wallace S, et al. Optimized orthogonal translation of unnatural amino acids enables spontaneous protein double-labelling and FRET. *Nat Chem.* 2014; 6(5):393–403. Epub 2014/04/24. <https://doi.org/10.1038/nchem.1919> PMID: 24755590.
23. Wang K, Schmied WH, Chin JW. Reprogramming the genetic code: from triplet to quadruplet codes. *Angew Chem Int Ed Engl.* 2012; 51(10):2288–97. Epub 2012/01/21. <https://doi.org/10.1002/anie.201105016> PMID: 22262408.
24. Fried SD, Schmied WH, Uttamapinant C, Chin JW. Ribosome Subunit Stapling for Orthogonal Translation in *E. coli*. *Angew Chem Int Ed Engl.* 2015; 54(43):12791–4. Epub 2015/10/16. <https://doi.org/10.1002/anie.201506311> PMID: 26465656.
25. Schmied WH, Tnimov Z, Uttamapinant C, Rae CD, Fried SD, Chin JW. Controlling orthogonal ribosome subunit interactions enables evolution of new function. *Nature.* 2018; 564(7736):444–8. Epub 2018/12/07. <https://doi.org/10.1038/s41586-018-0773-z> PMID: 30518861.
26. Orelle C, Carlson ED, Szal T, Florin T, Jewett MC, Mankin AS. Protein synthesis by ribosomes with tethered subunits. *Nature.* 2015; 524(7563):119–24. Epub 2015/07/30. <https://doi.org/10.1038/nature14862> PMID: 26222032.
27. Aleksashin NA, Szal T, d'Aquino AE, Jewett MC, Vazquez-Laslop N, Mankin AS. A fully orthogonal system for protein synthesis in bacterial cells. *Nat Commun.* 2020; 11(1):1858. Epub 2020/04/22. <https://doi.org/10.1038/s41467-020-15756-1> PMID: 32313034.
28. Youngman EM, Brunelle JL, Kochaniak AB, Green R. The active site of the ribosome is composed of two layers of conserved nucleotides with distinct roles in peptide bond formation and peptide release. *Cell.* 2004; 117(5):589–99. Epub 2004/05/28. [https://doi.org/10.1016/s0092-8674\(04\)00411-8](https://doi.org/10.1016/s0092-8674(04)00411-8) PMID: 15163407.
29. Thompson J, Kim DF, O'Connor M, Lieberman KR, Bayfield MA, Gregory ST, et al. Analysis of mutations at residues A2451 and G2447 of 23S rRNA in the peptidyltransferase active site of the 50S ribosomal subunit. *Proc Natl Acad Sci U S A.* 2001; 98(16):9002–7. Epub 2001/07/27. <https://doi.org/10.1073/pnas.151257098> PMID: 11470897.
30. d'Aquino AE, Azim T, Aleksashin NA, Hockenberry AJ, Kruger A, Jewett MC. Mutational characterization and mapping of the 70S ribosome active site. *Nucleic Acids Res.* 2020; 48(5):2777–89. Epub 2020/02/06. <https://doi.org/10.1093/nar/gkaa001> PMID: 32009164.
31. Murase Y, Nakanishi H, Tsuji G, Sunami T, Ichihashi N. In Vitro Evolution of Unmodified 16S rRNA for Simple Ribosome Reconstitution. *ACS Synth Biol.* 2018; 7(2):576–83. Epub 2017/10/21. <https://doi.org/10.1021/acssynbio.7b00333> PMID: 29053248.
32. Chen SS, Sperling E, Silverman JM, Davis JH, Williamson JR. Measuring the dynamics of *E. coli* ribosome biogenesis using pulse-labeling and quantitative mass spectrometry. *Mol Biosyst.* 2012; 8(12):3325–34. Epub 2012/10/24. <https://doi.org/10.1039/c2mb25310k> PMID: 23090316.
33. Sashital DG, Greeman CA, Lyumkis D, Potter CS, Carragher B, Williamson JR. A combined quantitative mass spectrometry and electron microscopy analysis of ribosomal 30S subunit assembly in *E. coli*. *Elife.* 2014; 3. Epub 2014/10/15. <https://doi.org/10.7554/eLife.04491> PMID: 25313868.
34. Kuhn E, Wu J, Karl J, Liao H, Zolg W, Guild B. Quantification of C-reactive protein in the serum of patients with rheumatoid arthritis using multiple reaction monitoring mass spectrometry and 13C-labeled peptide standards. *Proteomics.* 2004; 4(4):1175–86. Epub 2004/03/30. <https://doi.org/10.1002/pmic.200300670> PMID: 15048997.
35. Davydov II, Wohlgemuth I, Artamonova II, Urlaub H, Tonevitsky AG, Rodnina MV. Evolution of the protein stoichiometry in the L12 stalk of bacterial and organellar ribosomes. *Nat Commun.* 2013; 4:1387. Epub 2013/01/24. <https://doi.org/10.1038/ncomms2373> PMID: 23340427.
36. Kitagawa M, Ara T, Arifuzzaman M, Ioka-Nakamichi T, Inamoto E, Toyonaga H, et al. Complete set of ORF clones of *Escherichia coli* ASKA library (a complete set of *E. coli* K-12 ORF archive): unique resources for biological research. *DNA Res.* 2005; 12(5):291–9. Epub 2006/06/14. <https://doi.org/10.1093/dnares/dsi012> PMID: 16769691.
37. Datsenko KA, Wanner BL. One-step inactivation of chromosomal genes in *Escherichia coli* K-12 using PCR products. *Proc Natl Acad Sci U S A.* 2000; 97(12):6640–5. Epub 2000/06/01. <https://doi.org/10.1073/pnas.120163297> PMID: 10829079.

38. Pronobis MI, Deutch N, Peifer M. The Miraprep: A Protocol that Uses a Miniprep Kit and Provides Maxiprep Yields. *PLoS One*. 2016; 11(8):e0160509. Epub 2016/08/04. <https://doi.org/10.1371/journal.pone.0160509> PMID: 27486871.
39. Liu Y, Fritz BR, Anderson MJ, Schoborg JA, Jewett MC. Characterizing and alleviating substrate limitations for improved in vitro ribosome construction. *ACS Synth Biol*. 2015; 4(4):454–62. Epub 2014/08/01. <https://doi.org/10.1021/sb5002467> PMID: 25079899.
40. Pedelacq JD, Cabantous S, Tran T, Terwilliger TC, Waldo GS. Engineering and characterization of a superfolder green fluorescent protein. *Nat Biotechnol*. 2006; 24(1):79–88. Epub 2005/12/22. <https://doi.org/10.1038/nbt1172> PMID: 16369541.
41. Giansanti P, Tsiatsiani L, Low TY, Heck AJ. Six alternative proteases for mass spectrometry-based proteomics beyond trypsin. *Nat Protoc*. 2016; 11(5):993–1006. Epub 2016/04/29. <https://doi.org/10.1038/nprot.2016.057> PMID: 27123950.
42. Ishizuka N, Minakuchi H, Nakanishi K, Soga N, Nagayama H, Hosoya K, et al. Performance of a monolithic silica column in a capillary under pressure-driven and electrodriven conditions. *Anal Chem*. 2000; 72(6):1275–80. Epub 2000/03/31. <https://doi.org/10.1021/ac990942q> PMID: 10740870.
43. MacLean B, Tomazela DM, Shulman N, Chambers M, Finney GL, Frewen B, et al. Skyline: an open source document editor for creating and analyzing targeted proteomics experiments. *Bioinformatics*. 2010; 26(7):966–8. Epub 2010/02/12. <https://doi.org/10.1093/bioinformatics/btq054> PMID: 20147306.
44. Ban N, Beckmann R, Cate JH, Dinman JD, Dragon F, Ellis SR, et al. A new system for naming ribosomal proteins. *Curr Opin Struct Biol*. 2014; 24:165–9. Epub 2014/02/15. <https://doi.org/10.1016/j.sbi.2014.01.002> PMID: 24524803.
45. Moriya Y, Kawano S, Okuda S, Watanabe Y, Matsumoto M, Takami T, et al. The jPOST environment: an integrated proteomics data repository and database. *Nucleic Acids Res*. 2019; 47(D1):D1218–D24. Epub 2018/10/09. <https://doi.org/10.1093/nar/gky899> PMID: 30295851.
46. Charollais J, Pflieger D, Vinh J, Dreyfus M, Iost I. The DEAD-box RNA helicase SrmB is involved in the assembly of 50S ribosomal subunits in *Escherichia coli*. *Mol Microbiol*. 2003; 48(5):1253–65. Epub 2003/06/06. <https://doi.org/10.1046/j.1365-2958.2003.03513.x> PMID: 12787353.
47. Al-Majdoub ZM, Carroll KM, Gaskell SJ, Barber J. Quantification of the proteins of the bacterial ribosome using QconCAT technology. *J Proteome Res*. 2014; 13(3):1211–22. Epub 2014/02/06. <https://doi.org/10.1021/pr400667h> PMID: 24494973.
48. Aleksashin NA, Leppik M, Hockenberry AJ, Klepacki D, Vazquez-Laslop N, Jewett MC, et al. Assembly and functionality of the ribosome with tethered subunits. *Nat Commun*. 2019; 10(1):930. Epub 2019/02/26. <https://doi.org/10.1038/s41467-019-08892-w> PMID: 30804338.
49. Picotti P, Bodenmiller B, Aebersold R. Proteomics meets the scientific method. *Nat Methods*. 2013; 10(1):24–7. Epub 2012/12/28. <https://doi.org/10.1038/nmeth.2291> PMID: 23269373.
50. Picotti P, Aebersold R. Selected reaction monitoring-based proteomics: workflows, potential, pitfalls and future directions. *Nat Methods*. 2012; 9(6):555–66. Epub 2012/06/07. <https://doi.org/10.1038/nmeth.2015> PMID: 22669653.
51. Anderson L, Hunter CL. Quantitative mass spectrometric multiple reaction monitoring assays for major plasma proteins. *Mol Cell Proteomics*. 2006; 5(4):573–88. Epub 2005/12/08. <https://doi.org/10.1074/mcp.M500331-MCP200> PMID: 16332733.
52. Picotti P, Bodenmiller B, Mueller LN, Domon B, Aebersold R. Full dynamic range proteome analysis of *S. cerevisiae* by targeted proteomics. *Cell*. 2009; 138(4):795–806. Epub 2009/08/12. <https://doi.org/10.1016/j.cell.2009.05.051> PMID: 19664813.
53. Bourmaud A, Gallien S, Domon B. Parallel reaction monitoring using quadrupole-Orbitrap mass spectrometer: Principle and applications. *Proteomics*. 2016; 16(15–16):2146–59. Epub 2016/05/05. <https://doi.org/10.1002/pmic.201500543> PMID: 27145088.
54. Shilling PJ, Mirzadeh K, Cumming AJ, Widesheim M, Kock Z, Daley DO. Improved designs for pET expression plasmids increase protein production yield in *Escherichia coli*. *Commun Biol*. 2020; 3(1):214. Epub 2020/05/10. <https://doi.org/10.1038/s42003-020-0939-8> PMID: 32382055.
55. Shieh YW, Minguez P, Bork P, Auburger JJ, Guilbride DL, Kramer G, et al. Operon structure and cotranslational subunit association direct protein assembly in bacteria. *Science*. 2015; 350(6261):678–80. Epub 2015/09/26. <https://doi.org/10.1126/science.aac8171> PMID: 26405228.
56. Minton AP. Implications of macromolecular crowding for protein assembly. *Curr Opin Struct Biol*. 2000; 10(1):34–9. Epub 2000/02/19. [https://doi.org/10.1016/s0959-440x\(99\)00045-7](https://doi.org/10.1016/s0959-440x(99)00045-7) PMID: 10679465.
57. Ishihama Y, Rappsilber J, Mann M. Modular stop and go extraction tips with stacked disks for parallel and multidimensional Peptide fractionation in proteomics. *J Proteome Res*. 2006; 5(4):988–94. Epub 2006/04/11. <https://doi.org/10.1021/pr050385q> PMID: 16602707.

58. Pei H, Han S, Yang S, Lei Z, Zheng J, Jia Z. Phosphorylation of bacterial L9 and its functional implication in response to starvation stress. *FEBS Lett.* 2017; 591(20):3421–30. Epub 2017/09/13. <https://doi.org/10.1002/1873-3468.12840> PMID: 28898405.
59. Brown CW, Sridhara V, Boutz DR, Person MD, Marcotte EM, Barrick JE, et al. Large-scale analysis of post-translational modifications in *E. coli* under glucose-limiting conditions. *BMC Genomics.* 2017; 18(1):301. Epub 2017/04/18. <https://doi.org/10.1186/s12864-017-3676-8> PMID: 28412930.